Biochemical and Biophysical Research Communications 456 (2015) 66–73

Contents lists available at ScienceDirect

Biochemical and Biophysical Research Communications

journal homepage: www.elsevier.com/locate/ybbrc

# Chaperone protein HYPK interacts with the first 17 amino acid region of Huntingtin and modulates mutant HTT-mediated aggregation and cytotoxicity

Kamalika Roy Choudhury [a,b], Nitai P. Bhattacharyya [c,*]

[a] Crystallography & Molecular Biology Division, Saha Institute of Nuclear Physics, 1/AF Bidhannagar, Kolkata 700064, India
[b] Centre for Neuroscience, Indian Institute of Science, Bangalore 560012, India
[c] Biomedical Genomics Centre, PG Polyclinic Building, 5, Suburban Hospital Road, Kolkata 700020, India

ARTICLE INFO

*Article history:*
Received 22 October 2014
Available online 21 November 2014

*Keywords:*
Huntington's disease
HYPK
HTT-N17
Aggregate
Cytotoxicity

ABSTRACT

Huntington's disease is a polyglutamine expansion disorder, characterized by mutant HTT-mediated aggregate formation and cytotoxicity. Many reports suggests roles of N-terminal 17 amino acid domain of HTT (HTT-N17) towards subcellular localization, aggregate formation and subsequent pathogenicity induced by N-terminal HTT harboring polyQ stretch in pathogenic range. HYPK is a HTT-interacting chaperone which can reduce N-terminal mutant HTT-mediated aggregate formation and cytotoxicity in neuronal cell lines. However, how HYPK interacts with N-terminal fragment of HTT remained unknown. Here we report that specific interaction of HYPK with HTT-N17 is crucial for the chaperone activity of HYPK. Deletion of HTT-N17 leads to formation of tinier, SDS-soluble nuclear aggregates formed by N-terminal mutant HTT. The increased cytotoxicity imparted by these tiny aggregates might be contributed due to loss of interaction with HYPK.



## 1. Introduction

Huntington's disease (HD) is a neurodegenerative disorder caused by CAG repeat expansion in the Huntingtin (*HTT*) gene that encodes a polymorphic polyglutamine tract at the amino terminus of the Huntingtin protein. It was reported earlier that N-terminal HTT coded by exon1 of the *HTT* gene harboring more than 36 polyglutamine (polyQ) repeats are sufficient to form aggregates [1]. N-terminal HTT can be sub-divided into three regions: N-terminal 17 amino acid encoding domain (HTT-N17), polyQ domain and proline rich domain (PRD) at the end of the polyQ stretch. Several reports revealed that these polyQ flanking regions at N-terminal HTT coded by exon1 might influence aggregate formation and toxicity induced by the mutant protein (mHTT) [2–5]. Hundreds of proteins are identified to interact with HTT, especially with its N-terminal region; but only few have been shown to interact specifically with polyQ domain and PRD. Four proteins namely TPR [6], CRM1/Exportin1 [7], TRiC/CCT [8] and PACSIN1 [9] have specifically been reported to interact with HTT-N17.

The molecular chaperone TCP1 is a member of the chaperonin-containing TCP1 complex (CCT, also known as the TCP1 ring complex (TRiC)). TCP1 binds to the hydrophobic patches on HTT-N17 and inhibits formation of mHTT aggregates, possibly interfering with the folding back and interaction with itself and polyQ stretches. HTT-N17 is post-translationally modified (e.g. phosphorylated, sumoylated, etc.), but it is not clear whether these modifiers directly bind to this region [10–12]. The chaperone protein HYPK was reported earlier to reduce the aggregates of mHTT. Here we intend to check whether the mechanism of action of HYPK could be similar to TRiC and report for the first time that HYPK interacts with HTT-N17 and modulate the cytotoxicity induced by mutant HTT in neuronal cell lines.

## 2. Materials and methods

### 2.1. Mammalian cell culture and transfection

Immortalized striatal HD control cell line (ST$Hdh^{Q7}$/$Hdh^{Q7}$) were gifted by Dr. Marcy E. MacDonald, Massachusetts General Hospital, USA. Mouse neuroblastoma cell lines, Neuro2A, were procured

* Corresponding author at: Crystallography & Molecular Biology Division, Saha Institute of Nuclear Physics, 1/AF Bidhannagar, Kolkata 700064, India. Fax: +91 33 2337 4637.
*E-mail addresses:* nitai_sinp@yahoo.com, director.bmgc@nibmg.ac.in (N.P. Bhattacharyya).

http://dx.doi.org/10.1016/j.bbrc.2014.11.035
0006-291X/

from NCCS, Pune, India. All cells were cultured and transfected as mentioned earlier [13].

### 2.2. Cloning of HTT exon1 deletion constructs

16Q-DsRed and 83Q-DsRed (*HTT* exon1 harboring 16 and 83 CAG repeats, respectively, cloned in DsRed) were overexpressed in ST$Hdh^{Q7}$/$Hdh^{Q7}$ and Neuro2A cells to mimic HD phenotypes like aggregate formation and apoptosis.

Following primers were designed for cloning various deletion constructs of N-terminal mutant *HTT* (83Q-DsRed used as template for PCR)

83QΔN17-DsRed_F: 5′-ACGCGTCGACGTATGCAGCAGCAGCAG-CAGC-3′
83QΔN17-DsRed_R: 5′-TGGGATCCGGTCGGTGCAGCGGCTCCT-CAGC-3′
83QΔPRD-DsRed_F: 5′-ACGCGTCGACGTCATGGCGACCCTG-GAAAGCT GAT-3′
83QΔPRD-DsRed_R: 5′-CGGGATCCCCGGGCGGTGGCGGCTGT-TG-3′
HTT-N17-DsRed_F: 5′-ACGCGTCGACGTATGGCGACCCTGGA-AAA-3′
HTT-N17-DsRed_R: 5′-CGGGATCCGAAGGACTTGAGGGACTCG-AA-3′.

### 2.3. Confocal imaging and FRAP experiments

Co-localization of proteins was determined using confocal microscopy following methods described earlier [14]. Extent of co-localization between the pixels of the two channels was determined by average of square of the Pearson correlation coefficient values ($R^2$) of 10 random cells in the field. Nucleus staining was performed using DAPI solution at a final concentration of 0.1 μg/ml. Neuro2A cells were transfected with 500 ng of 83Q-DsRed, 83QΔN17-DsRed, 83QΔPRD-DsRed or HTT-N17-DsRed and percentage of cells containing aggregates was determined using confocal microscope and plotted. Fluorescence recovery after photobleaching (FRAP) experiments were performed and relative fluorescence intensities (RFI) at each time point were calculated following standard methods [14].

### 2.4. Co-immunoprecipitation (co-IP) and western blot analysis

Cells in culture were washed and scraped with 1 ml of ice-cold PBS and collected by centrifugation at 4500 rpm for 3 min at 4 °C. We prepared cell lysates and performed co-immunoprecipitation (co-IP) following methods published earlier [13]. Anti-DsRed antibody was used to immunoprecipitate the N-terminal mHTT complex. Following antibodies were used to analyze immune complexes after co-IP or to detect presence of polyQ and HYPK following filter retardation:

Rabbit anti-HYPK: Sigma polyclonal, Cat No. SAB1101780
Rabbit anti-DsRedC1: Clontech polyclonal, Cat No. 632496
Mouse anti-polyQ: Chemicon, CA, USA, Cat No. MAB1574.

### 2.5. Filter retardation assay

For filter retardation, Neuro2A cells were transfected with 83Q-DsRed or 83QΔN17-DsRed constructs. After 48 h of transfection, cells were harvested and protein was prepared by centrifugation at 13,000 rpm for 15 min at 4 °C. The resulting pellet was treated and subjected to filter retardation experiment following methods described earlier [15]. Presence of 83Q and HYPK on the membrane was probed in a dose-responsive manner (10 μg and 40 μg) using anti-polyQ and anti-HYPK antibodies. To probe more than one protein on the same blot, we stripped and reprobed PVDF membrane [13].

### 2.6. Cell survival (MTT assay) in presence and absence of HYPK

MTT assay was performed to measure cell survival in particular conditions following methods described earlier [13].

### 2.7. Statistical analysis and artwork preparation

All experiments were repeated at least thrice unless otherwise mentioned and mean values, standard deviations and $p$ values for Student's unpaired two-tailed $t$ tests were calculated. Microsoft Excel and GraphPadQuickCalcs softwares were used for data analyses. All artworks were prepared using Adobe Photoshop CS3.

## 3. Results

### 3.1. Deletion constructs of mutant HTT exon1 and their sub-cellular localizations

We prepared N-terminal mHTT constructs by deleting sequences coding for the first 17 amino acid and PRD (designated as 83QΔN17-DsRed and 83QΔPRD-DsRed respectively). Sequence that codes only the first 17 amino acids was also cloned in DsRed vector (designated as HTT-N17-DsRed). All constructs are pictorially represented in Fig. 1, panel A. We overexpressed 83Q-DsRed, 83QΔN17-DsRed or 83QΔPRD-DsRed in Neuro2A cells for 48 h and detected their expressions using confocal microscopy. In Neuro2A cells, overexpression of 83Q-DsRed and 83QΔPRD-DsRed resulted in formation of aggregates mostly in perinuclear region, whereas aggregates formed by 83QΔN17-DsRed were identified exclusively in cell nucleus (Fig. 1, panel B).

### 3.2. Aggregates formed by N-terminal mutant HTT with 83Q-DsRed and its deletion mutants

We counted the visible aggregates formed by all N-terminal mHTT constructs 48 h post-transfection. Although 83QΔN17-DsRed aggregates were solely nuclear and apparently smaller in size (Fig. 1, panel B), there was no statistically significant difference in percentage of cells bearing aggregates formed by 83Q-DsRed and 83QΔN17-DsRed (61.3 ± 9.7% and 58.3 ± 9.5% respectively, $p = 0.7214$, $n = 3$) (Fig. 2, panel A). Percentage of 83QΔPRD-DsRed expressing cells containing aggregates was 41.7 ± 3.1; significantly less as compared to aggregates formed by 83Q-DsRed overexpression ($p = 0.03$, $n = 3$). We further observed that cells expressing HTT-N17-DsRed formed visible aggregates in only 1.7 ± 1.2% cells, significantly less as compared to 83Q-DsRed ($p = 0.0005$, $n = 3$) (Fig. 2, panel A).

### 3.3. Size and nature of aggregates formed by 83Q-DsRed and its deletion constructs in Neuro2A

Using confocal microscope, we observed that out of 100 cells in field, 17 cells expressing 83Q-DsRed and 22 cells expressing 83QΔPRD-DsRed contained aggregates in the range of >10 to 16 μm. However, only 3 cells expressing 83QΔN17-DsRed formed aggregates in this size range. There were 3 83Q-DsRed expressing cells with aggregate size >20 μm. However, no cell overexpressing 83QΔPRD-DsRed or 83QΔN17-DsRed was found having aggregates in these high size range. Aggregates formed by 83QΔN17-DsRed were significantly smaller than those induced by 83Q-DsRed. Nine

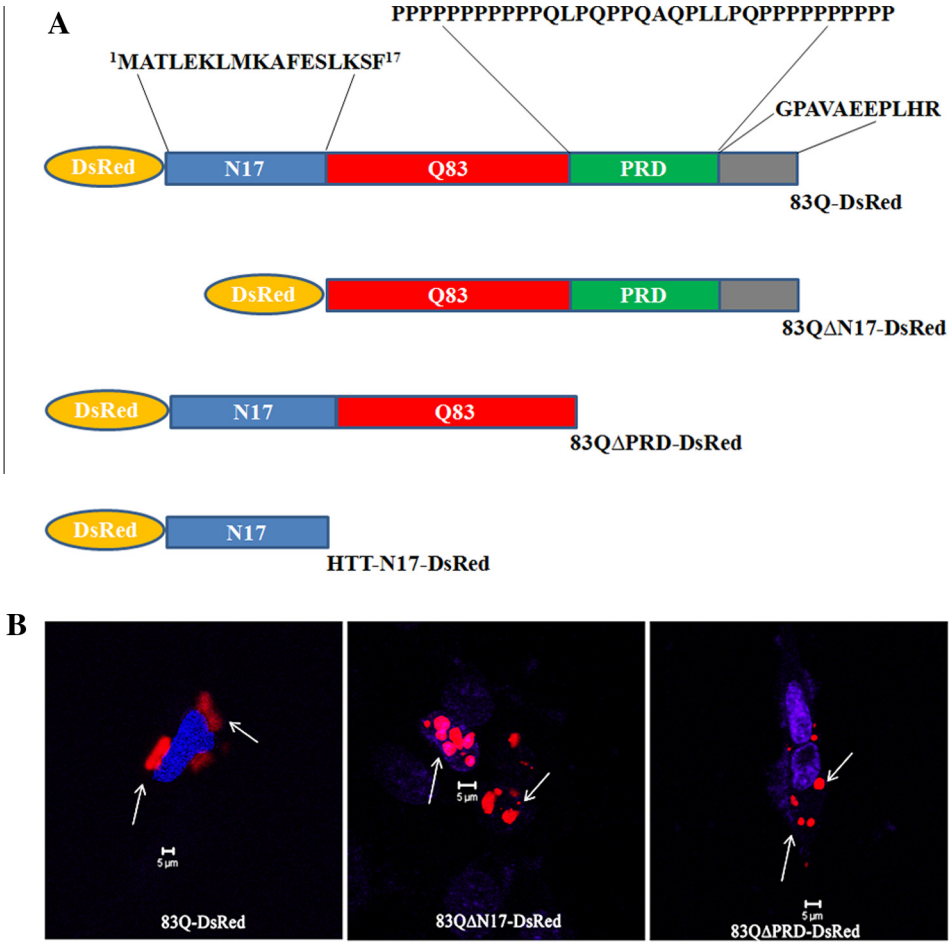


**Fig. 1. 83Q-DsRed and its deletion mutants**. Panel A represents 83Q and its different deletion mutants cloned in DsRed vector. Constructions of full length exon1 with 83 glutamine stretch (83Q), 83QΔN17 (deletion of N17 region), HTT exon1 harboring N17 and 83Q, but no PRD (83QΔPRD-DsRed) and HTT-N17-DsRed (devoid of polyQ region and PRD) are shown. Localization of aggregates induced by 83Q-DsRed, 83QΔN17-DsRed and 83QΔPRD-DsRed are shown in panel B. Cell nuclei are stained with DAPI. 5 μm scale bars are included in the confocal images.

83QΔN17-DsRed expressing cells were even observed to form aggregates in the size range of 1–4 μm (Fig. 2, panel B).

From FRAP experiments of 83Q-DsRed, 83QΔN17-DsRed and 83QΔPRD-DsRed aggregates in Neuro2A cells, it was observed that fluorescence intensity of the aggregates formed by 83Q-DsRed did not recover within 1 min after photobleaching, indicating that these aggregates were quite tight and insoluble. The mobile fraction of 83Q-DsRed aggregates was calculated to be only 0.35. Similar nature of the aggregates formed by 83QΔPRD-DsRed was observed and the soluble fraction was calculated to be 0.41. On the contrary, fluorescence intensity of the small nuclear aggregates formed by 83QΔN17-DsRed constructs recovered within 1 min of photobleaching, with a soluble fraction of 0.61 (Fig. 2, panel C). This result revealed that 83QΔN17-DsRed aggregates were more soluble or diffused than aggregates formed by 83Q-DsRed or 83QΔPRD-DsRed.

### 3.4. Cytotoxicity induced by different deletion mutants of N-terminal mHTT

To determine ability of these mHTT deletion constructs in inducing cytotoxicity, we performed MTT cell survival assay upon transfection of Neuro2A cells with 16Q-DsRed, 83Q-DsRed, HTT-N17-DsRed, 83QΔPRD-DsRed or 83QΔN17-DsRed. Fraction survival of Neuro2A cells overexpressing 16Q-DsRed was found to be 0.89 ± 0.08, which dropped significantly to 0.60 ± 0.02 ($p = 0.03$, $n = 3$) upon 83Q-DsRed overexpression. HTT-N17-DsRed did not show toxicity (percent cell survival was 0.90 ± 0.1). Cells expressing either 83QΔN17-DsRed or 83QΔPRD-DsRed exhibited decreased survival, 0.51 ± 0.03% and 0.68 ± 0.04%, respectively. Results are graphically represented in Fig. 2, panel D and summary of the results and level of significances between two conditions are shown in Table 1.

### 3.5. Interaction of HYPK with 83Q-DsRed and different deletion mutants

Coexpression of HYPK-GFP (cloned earlier [14]) and 83Q-DsRed in $STHdh^{Q7}/Hdh^{Q7}$ cells and visualization under confocal microscope 48 h post-transfection revealed that both were co-localized throughout the cells, mainly in cell cytoplasm. No visible aggregate was found in this condition. Coexpression of HYPK-GFP with other deletion constructs revealed that HYPK co-localized with HTT-N17-DsRed and 83QΔPRD-DsRed mainly in cytoplasm and not with 83QΔN17-DsRed (Fig. 3, panel A). $R^2$ values for interaction of HYPK-GFP with 83Q-DsRed, 83QΔPRD-DsRed, 83QΔN17-DsRed and HTT-N17-DsRed were 0.87, 0.76, 0.31 and 0.65, respectively. Interestingly, 83QΔN17-DsRed formed mostly nuclear aggregates whereas the 83QΔPRD-DsRed aggregates were mostly cytoplasmic. We further confirmed such interactions by co-IP. $STHdh^{Q7}/Hdh^{Q7}$ cells were transfected with 83Q-DsRed or the deletion constructs. After 48 h of transfection, cell lysates was extracted and

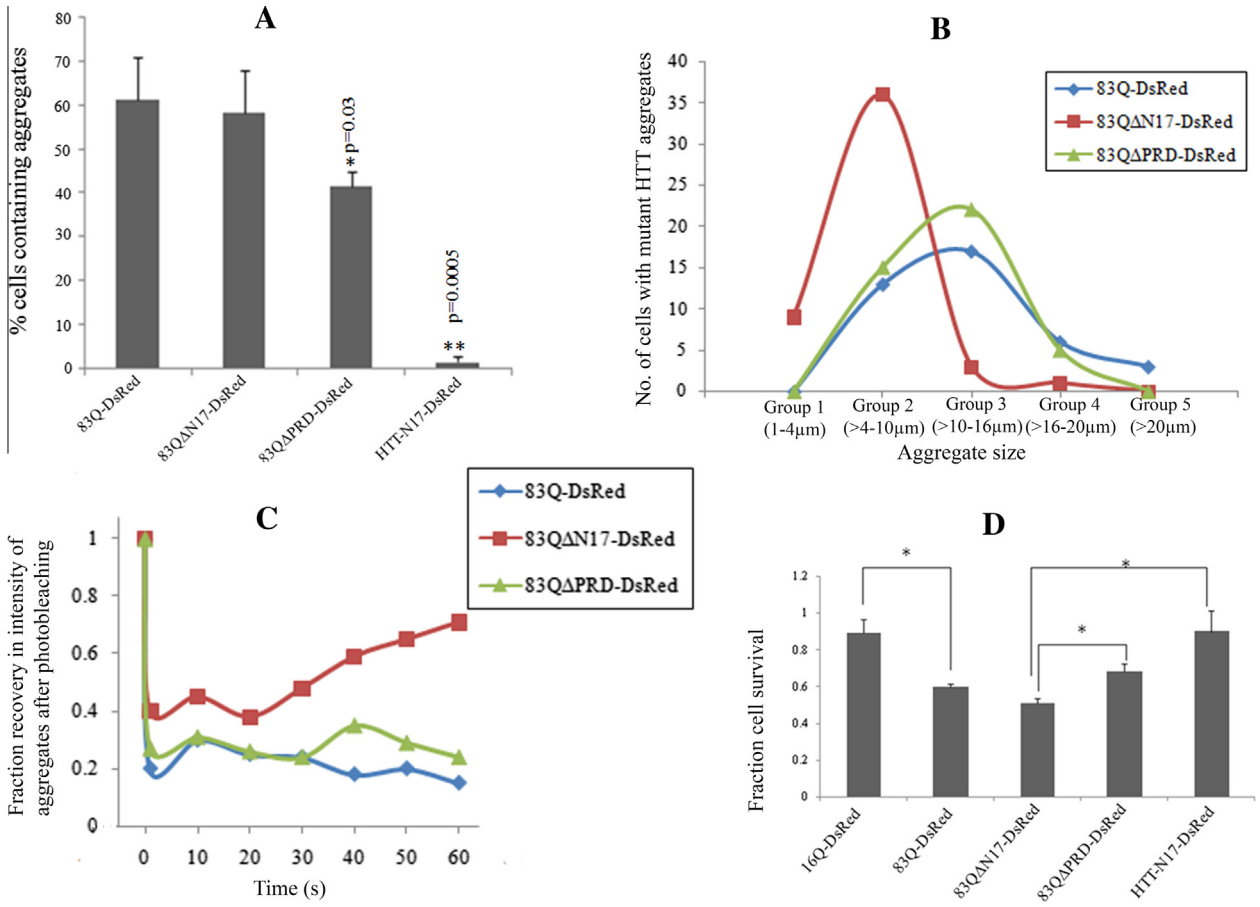


**Fig. 2. Nature and size of aggregates formed by deletion constructs of N-terminal mHTT**. Percentage of Neuro2A cells harbouring aggregates counted upon overexpression of 83Q-DsRed, 83QΔN17-DsRed, 83QΔPRD-DsRed and HTT-N17-DsRed (panel A). Size distribution of 83Q-DsRed aggregates in presence and absence of N17 and PRD domains (panel B). 83Q-DsRed and 83QΔPRD-DsRed aggregates mostly fall in the range of >10–16 μm, whereas 83QΔN17-DsRed formed maximum No. of aggregates in >4–10 μm range (panel B). FRAP experiments comparing recovery in fluorescence intensities of 83QΔN17-DsRed and 83QΔPRD-DsRed with 83Q-DsRed aggregates after photobleaching (panel C). Results obtained with 83Q-DsRed, 83QΔN17-DsRed and 83QΔPRD-DsRed are represented by blue, red and green curves respectively in panels B and C. Effects of overexpression of 16Q, 83Q and various deletion mutants on Neuro2A cell survival (panel D). Results are mean ± standard deviation of three or more independent experiments with p values for Student's unpaired two-tailed *t* test.

**Table 1**
**Survival of Neuro2A cells expressing various constructs of N-terminal HTT.**

| Serial No. | Constructs | Cell survival | Compared between | Comments and level of significance |
|---|---|---|---|---|
| 1 | 16Q-DsRed | 0.89 ± 0.08 | 1 and 2<br>1 and 3<br>1 and 4<br>1 and 5 | Decrease, $p = 0.003$<br>Decrease, $p = 0.001$<br>Decrease, $p = 0.01$<br>Unchanged, $p = 0.93$ |
| 2 | 83Q-DsRed | 0.60 ± 0.02 | 2 and 3<br>2 and 4<br>2 and 5 | Decreased, $p = 0.009$<br>Increased, $p = 0.03$<br>Increased, $p = 0.01$ |
| 3 | 83QΔN17-DsRed | 0.51 ± 0.03 | 3 and 4<br>3 and 5 | Increased, $p = 0.004$<br>Increased, $p = 0.005$ |
| 4 | 83QΔPRD-DsRed | 0.68 ± 0.04 | 4 and 5 | Increased, $p = 0.004$ |
| 5 | HTT-N17-DsRed | 0.90 ± 0.1 | – | – |

mHTT protein complex were pulled using anti-DsRed antibody and presence of endogenous HYPK in this complex was detected using anti-HYPK antibody. The blots were stripped and reprobed with anti-DsRed antibody to show the presence of N-terminal mHTT variants in these complexes (Fig. 3, panel B). The results confirmed that endogenous HYPK interacted with 83Q-DsRed, 83QΔPRD-DsRed and HTT-N17-DsRed but could not interact with N-terminal mHTT upon deletion of HTT-N17.

### *3.6. Effects of HYPK on cytotoxicity induced by different deletion mutants of 83Q-DsRed*

As observed from Fig. 2, panel D the order of survival of Neuro2A cells overexpressing 83Q or its deletion mutants was 83QΔPRD-DsRed > 83Q-DsRed > 83QΔN17-DsRed. We have shown that HYPK interacts with 83Q and 83QΔPRD constructs, but failed to interact with the N-terminal mHTT when HTT-N17

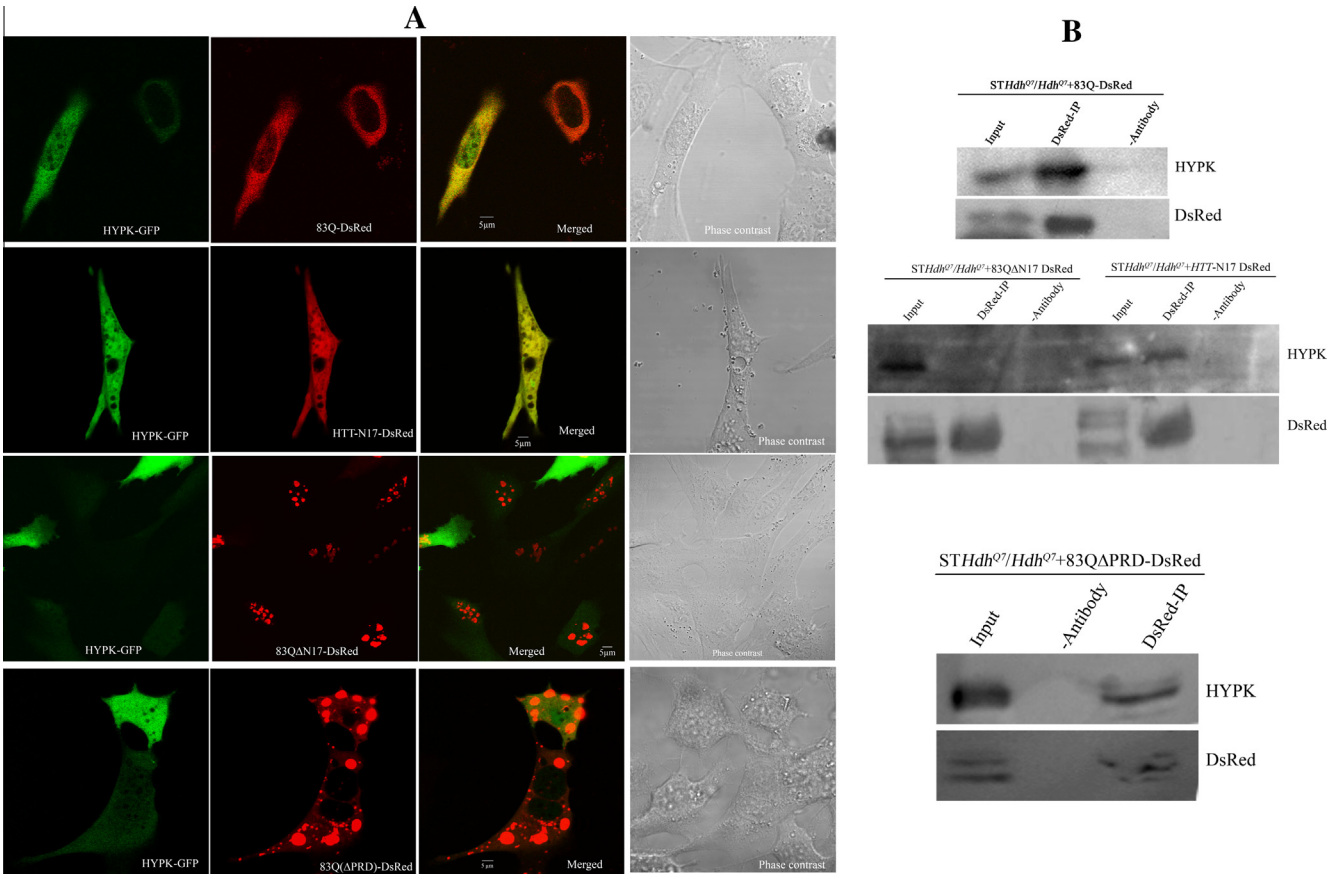


**Fig. 3. Interaction of HYPK-GFP with 83Q-DsRed and its deletion mutants**. Panel A shows co-localizations of 83Q-DsRed, HTT-N17-DsRed, 83QΔN17-DsRed and 83QΔPRD-DsRed with HYPK-GFP. In panel B, co-IP of 83Q and these deletion constructs with HYPK is shown. Anti-DsRed primary antibody was used to immunoprecipitate and anti-HYPK antibody was used to detect presence of HYPK in the N-terminal mHTT immune complex. Blots reprobed with anti-DsRed to confirm presence of mHTT in the immune complex. Scale bar of 5 μm for confocal images are included.

**Table 2**
**Effects of HYPK-DsRed on survival of Neuro2A cells expressing 16Q-DsRed, 83Q-DsRed, 83QΔN17-DsRed, 83QΔPRD-DsRed or HTT-N17-DsRed.**

| Serial No. | Constructs | Cell survival | Compared between | Level of significance |
|---|---|---|---|---|
| 1 | 16Q-DsRed | 0.89 ± 0.08 | 1 and 6 | Unchanged, $p = 0.81$ |
| 2 | 83Q-DsRed | 0.60 ± 0.02 | 2 and 7 | Increased, $p = 0.0001$ |
| 3 | 83QΔN17-DsRed | 0.51 ± 0.03 | 3 and 8 | Increased, $p = 0.08$ |
| 4 | 83QΔPRD-DsRed | 0.68 ± 0.04 | 4 and 9 | Increased, $p = 0.007$ |
| 5 | HTT-N17-DsRed | 0.90 ± 0.1 | 5 and 10 | Unchanged, ($p = 0.94$) |
| 6 | 16Q-DsRed & HYPK-DsRed | 0.91 ± 0.06 | – | – |
| 7 | 83Q-DsRed & HYPK-DsRed | 0.94 ± 0.04 | – | – |
| 8 | 83QΔN17-DsRed & HYPK-DsRed | 0.55 ± 0.006 | – | – |
| 9 | 83QΔPRD-DsRed & HYPK-DsRed | 0.88 ± 0.05 | – | – |
| 10 | HTT-N17-DsRed & HYPK-DsRed | 0.91 ± 0.07 | – | – |

was deleted (83QΔN17) (Fig. 3). To check whether interaction of N-terminal mHTT with HYPK has any biological relevance, we overexpressed 16Q-DsRed, 83Q-DsRed, 83QΔN17-DsRed, 83QΔPRD-DsRed or HTT-N17-DsRed in presence of HYPK-DsRed in Neuro2A cells. Result of this experiment is summarized in Table 2 and graphically represented in Fig. 4, panel A. Exogenous expression of HYPK was able to significantly recover the survival of cells expressing 83Q-DsRed ($p = 0.0001$, $n = 3$) from 0.60 ± 0.02 to 0.94 ± 0.04. Similarly, significant increase in survival by exogenous HYPK was also observed in cells expressing 83QΔPRD-DsRed (0.68 ± 0.04 to 0.88 ± 0.05, $p = 0.007$, $n = 3$). Interestingly, the effect of exogenous HYPK on survival of Neuro2A overexpressing 83QΔN17-DsRed was statistically insignificant (0.51 ± 0.03 to 0.55 ± 0.006, $p = 0.08$, $n = 3$).

### 3.7. Effects of HYPK on SDS-solubility of N-terminal mHTT aggregates

We performed filter retardation experiments with 10 μg and 40 μg Neuro2A cell lysates overexpressing 83Q-DsRed or 83QΔN17-DsRed. After trapping the SDS-insoluble aggregates, we probed the membrane with anti-polyQ or anti-HYPK antibodies. SDS-insoluble polyQ aggregates were visible in Neuro2A lysates overexpressing 83Q-DsRed (Fig. 4, panel B). On the contrary, we failed to find insoluble polyglutamine aggregates in

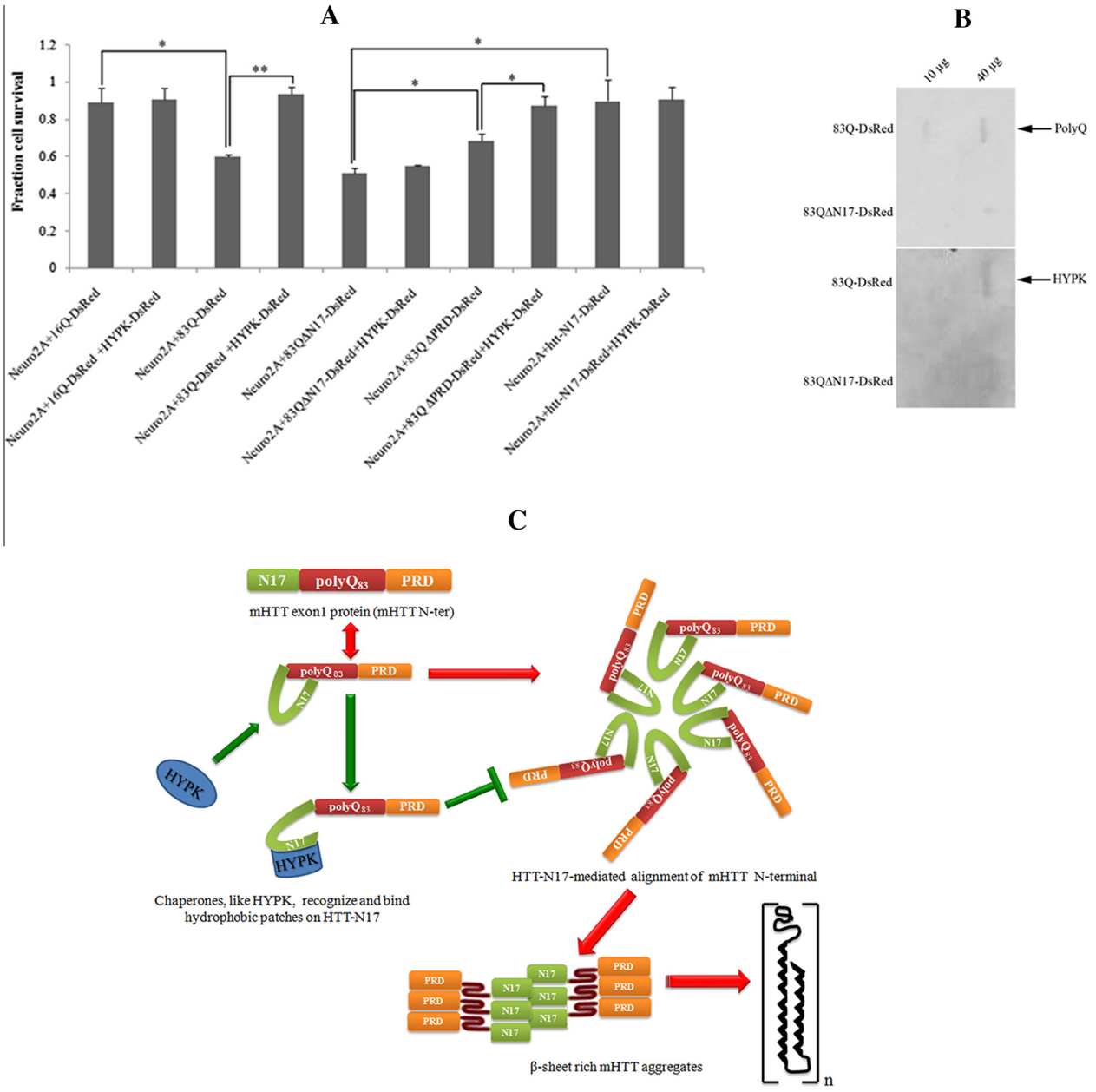


**Fig. 4. HYPK in recovery of mHTT-mediated cell death and aggregate formation**. Recovery in survival of Neuro2A cells overexpressing 83Q-DsRed, 83QΔN17-DsRed and 83Q-ΔPRD-DsRed were calculated and plotted (panel A). SDS-solubility of 83QΔN17-DsRed and 83Q-DsRed aggregates using filter retardation assay. Presence of HYPK in 83Q-DsRed and in 83QΔN17-DsRed aggregates also checked in a dose responsive manner (panel B). Probable model for inhibition of mHTT (83Q) aggregate formation by HYPK shown in panel C. HTT-N17 interacts with itself (homotypic interaction) and folds back on polyQ domain and stimulate alignment of N-terminal mHTT fragment, ultimately leading to formation of β-sheet rich aggregated structures (pathway shown by red arrows). We propose that HYPK might interact with HTT-N17 and mask these regions crucial for alignment, thus suppressing aggregate formation (pathway shown in green arrows). (For interpretation of the references to color in this figure legend, the reader is referred to the web version of this article.)

lysates extracted from Neuro2A cells overexpressing 83QΔN17-DsRed. It is interesting to recapitulate here that tiny visible nuclear aggregates induced by 83QΔN17-DsRed was observed under confocal microscope (Fig. 1, panel B). These small 83QΔN17-DsRed aggregates, therefore, were found to be more soluble; concomitant to our observation from the FRAP assay (Fig. 2, panel C). These results indicated that the visible nuclear aggregates formed in cells expressing 83QΔN17-DsRed were not amyloid-like fibrils of mHTT as observed in cells expressing 83Q-DsRed, rather were more soluble structures (Fig. 4, panel B). To check whether HYPK associates with the soluble mHTT or with the SDS-insoluble aggregates, we reprobed the blot with anti-HYPK antibody and observed association of HYPK only with the SDS-insoluble 83Q-DsRed aggregates (in 40 µg load, Fig. 4, panel B).

### *3.8. Localizations of other HTT-interacting chaperones with 83Q-DsRed and its deletion mutants*

We further tested whether some HTT-interacting proteins (mostly chaperones) localize with mHTT similar to HYPK. To this end, we cotransfected 83QΔN17-DsRed, 83QΔPRD-DsRed or HTT-N17-DsRed with the GFP tagged HTT-interacting proteins viz., HSPA1A, HSPB1, HCG3, MLF1 and MLF2 (all constructs previously cloned in our lab). The confocal microscope images for co-

localization between 83QΔN17-DsRed and these HTT-interacting partners are provided in Supplementary Fig. S1, panel A. As observed from the co-localization data, except for MLF2-GFP ($R^2$ value 0.76 with 83QΔN17 aggregates), none of these HTT-interacting chaperones co-localized with 83QΔN17-DsRed (Supplementary Fig. S1, panel A). Association between MLF2-GFP and 83QΔN17-DsRed was also confirmed by co-IP. We further tested co-localization of these HTT-interacting chaperones with HTT-N17-DsRed (Supplementary Fig. S1, panel B) and 83QΔPRD-DsRed (Supplementary Fig. S1, panel C). As observed from panel B, all HTT-chaperones (except for MLF2-GFP) co-localized significantly with HTT-N17-DsRed. All of these proteins also co-localized with 83QΔPRD-DsRed (Supplementary Fig. S1, panel C). $R^2$ values are provided in Supplementary Table 1.

## 4. Discussions

PolyQ flanking sequences on N-terminal mutant HTT were widely reported as modulators of HTT sub-cellular localization and mutant HTT-mediated aggregation and cytotoxicity [7,16]. It was reported earlier that point mutation M8P at HTT-N17 disrupts the structure of this peptide and lead to nuclear localization, resulting in no visible aggregate formation but significantly increasing cytotoxicity [17]. Whether deletion of the entire length of HTT-N17 or mutation at a single amino acid (M8P) alter the ability to form aggregates remains unclear, however, in both cases N-terminal mHTT localizes in cell nuclei, possibly due to change in the nuclear export ability; which might be contributed by interaction with proteins involved in nuclear export [6,17]. Deletion of PRD was also reported to reduce aggregate formation by mHTT in cell culture [18] and *in vitro* with synthetic peptide [4].

Our confocal and FRAP experiments confirmed that even though the number of cells containing aggregates induced by 83Q-DsRed and 83QΔN17-DsRed were similar, the sub-cellular localizations, sizes and the nature of the aggregates formed in these two cases varied completely. Aggregates formed by 83QΔN17-DsRed were significantly smaller in size, nuclear and loose. Upon expression of 83QΔN17-DsRed cell survival reduced significantly; even more than reduced by 83Q-DsRed. This result indicated that HTT-N17 protects cells from toxic consequences of N-terminal mHTT to some extent, possibly by exporting them from nucleus to cytoplasm. It also supports the hypothesis that nuclear aggregates are much more toxic [17], even though they are smaller in sizes and more mobile. On the contrary, deletion of PRD at least partially provides protection as the survival fraction was marginally but significantly higher in cells expressing 83QΔPRD-DsRed compared to that in cells expressing 83Q-DsRed. Although we observed a marginal increase in survival of Neuro2A cells expressing 83QΔN17 by HYPK that could be due to effects of HYPK on other biological processes which in turn influence cell survival.

The molecular chaperone TRiC was observed earlier to interact with HTT-N17, suppressing aggregate formation and cytotoxicity induced by the N-terminal mHTT [19]. Therefore, we asked whether the chaperone protein HYPK that suppress mutant HTT-mediated aggregate formation in cell line similarly interacts with HTT-N17. Our co-IP experiment confirmed that HYPK specifically interact with HTT-N17. In presence of exogenous HYPK and N-terminal mHTT, no visible aggregates were observed, while cells coexpressing 83QΔPRD-DsRed and HYPK-GFP formed visible aggregates; indicating that HTT-PRD might influence such interaction with HYPK and subsequent reduction in aggregate formation. In this study, we also observed that besides HYPK, other HTT-interacting proteins like HSPA1A, HSPB1, HCG3 and MLF1 but not MLF2 co-localized with HTT-N17. Whether these HTT-chaperones share similar interaction patterns demand further study.

It has been observed earlier that the amyloid-like fibrils of mutant HTT are SDS-insoluble and heat stable. These mHTT fibrils were considered as pathogenic causes behind HD [20]. On the contrary, recent findings suggest that soluble oligomers are also common to most amyloid formation and might represent the primary toxic species of amyloid [21]. Some consider SDS-soluble oligomeric intermediate structure to be the main factor behind HD pathology [22,23]. We performed filter retardation experiment and observed that aggregates induced by 83Q-DsRed was SDS-insoluble, whereas those formed by 83QΔN17-DsRed were SDS-soluble. HYPK only associated with these 83Q-DsRed aggregates, and not with 83QΔN17-DsRed aggregates. Together, the results observed from MTT and filter retardation assay suggested that the SDS-soluble aggregates formed by the 83QΔN17-DsRed constructs were more cytotoxic than the full length N-terminal mHTT construct, 83Q-DsRed. Whether these tinier aggregates are oligomers remain an open question.

To conclude, here for the first time we report that HTT-N17 domain is indispensible for interaction with HYPK, an HTT-interacting intrinsically disordered chaperone. However, interaction of HTT N-terminal fragment with HYPK might take place in absence of HTT-PRD also. Our results corroborate the findings of other groups regarding effect of HTT-N17 on nuclear export, cytotoxicity and aggregate formation [7,16]. Additionally we here report that 83QΔN17 aggregates are SDS-soluble and possibly due to lack of interaction between HYPK and 83QΔN17, overexpression of HYPK in neuronal cells could neither significantly recover aggregate formation nor reduce cytotoxicity induced by 83QΔN17 construct. Similar to the proposed model by Liebman et al. [24] and Tam et al. [19], we propose here that interaction of HYPK (and possibly other HTT-interacting chaperones) with HTT-N17 might inhibit HTT-N17 homotypic interactions and interaction of pathogenic polyQ tract on HTT with this amphipathic, alpha-helical region. This, in turn, might reduce aggregate formation and cytotoxicity, two major hallmarks of HD pathology (represented in Fig. 4, panel C).

## Conflict of interest

The authors declare no conflict of interest.

## Acknowledgment

The authors acknowledge Department of Atomic Energy, Govt. of India for funding this work.

## Appendix A. Supplementary data

Supplementary data associated with this article can be found, in the online version, at http://dx.doi.org/10.1016/j.bbrc.2014.11.035.

## References

[1] L. Mangiarini, K. Sathasivam, M. Seller, B. Cozens, A. Harper, C. Hetherington, M. Lawton, Y. Trottier, H. Lehrach, S.W. Davies, G.P. Bates, Exon 1 of the HD gene with an expanded CAG repeat is sufficient to cause a progressive neurological phenotype in transgenic mice, Cell 87 (1996) 493–506.
[2] D. Bulone, L. Masino, D.J. Thomas, P.L. San Biagio, A. Pastore, The interplay between PolyQ and protein context delays aggregation by forming a reservoir of protofibrils, PLoS ONE 1 (2006) e111.
[3] M. Jayaraman, R. Kodali, B. Sahoo, A.K. Thakur, A. Mayasundari, R. Mishra, C.B. Peterson, R. Wetzel, Slow amyloid nucleation via alpha-helix-rich oligomeric intermediates in short polyglutamine-containing Huntingtin fragments, J. Mol. Biol. 415 (2012) 881–899.
[4] A. Bhattacharyya, A.K. Thakur, V.M. Chellgren, G. Thiagarajan, A.D. Williams, B.W. Chellgren, T.P. Creamer, R. Wetzel, Oligoproline effects on polyglutamine conformation and aggregation, J. Mol. Biol. 355 (2006) 524–535.
[5] Z. Ignatova, A.K. Thakur, R. Wetzel, L.M. Gierasch, In-cell aggregation of a polyglutamine-containing chimera is a multistep process initiated by the flanking sequence, J. Biol. Chem. 282 (2007) 36736–36743.

[6] J. Cornett, F. Cao, C.E. Wang, C.A. Ross, G.P. Bates, S.H. Li, X.J. Li, Polyglutamine expansion of Huntingtin impairs its nuclear export, Nat. Genet. 37 (2005) 198–204.
[7] T. Maiuri, T. Woloshansky, J. Xia, R. Truant, The Huntingtin N17 domain is a multifunctional CRM1 and Ran-dependent nuclear and cilial export signal, Hum. Mol. Genet. (2013).
[8] S. Tam, R. Geller, C. Spiess, J. Frydman, The chaperonin TRiC controls polyglutamine aggregation and toxicity through subunit-specific interactions, Nat. Cell Biol. 8 (2006) 1155–1162.
[9] N.S. Caron, C.R. Desmond, J. Xia, R. Truant, Polyglutamine domain flexibility mediates the proximity between flanking sequences in Huntingtin, Proc. Natl. Acad. Sci. U.S.A. 110 (2013) 14610–14615.
[10] C.T. Aiken, J.S. Steffan, C.M. Guerrero, H. Khashwji, T. Lukacsovich, D. Simmons, J.M. Purcell, K. Menhaji, Y.Z. Zhu, K. Green, F. Laferla, L. Huang, L.M. Thompson, J.L. Marsh, Phosphorylation of threonine 3: implications for Huntingtin aggregation and neurotoxicity, J. Biol. Chem. 284 (2009) 29427–29436.
[11] J.S. Steffan, N. Agrawal, J. Pallos, E. Rockabrand, L.C. Trotman, N. Slepko, K. Illes, T. Lukacsovich, Y.Z. Zhu, E. Cattaneo, P.P. Pandolfi, L.M. Thompson, J.L. Marsh, SUMO modification of Huntingtin and Huntington's disease pathology, Science 304 (2004) 100–104.
[12] L.M. Thompson, C.T. Aiken, L.S. Kaltenbach, N. Agrawal, K. Illes, A. Khoshnan, M. Martinez-Vincente, M. Arrasate, J.G. O'Rourke, H. Khashwji, T. Lukacsovich, Y.Z. Zhu, A.L. Lau, A. Massey, M.R. Hayden, S.O. Zeitlin, S. Finkbeiner, K.N. Green, F.M. LaFerla, G. Bates, L. Huang, P.H. Patterson, D.C. Lo, A.M. Cuervo, J.L. Marsh, J.S. Steffan, IKK phosphorylates Huntingtin and targets it for degradation by the proteasome and lysosome, J. Cell Biol. 187 (2009) 1083–1099.
[13] K.R. Choudhury, S. Raychaudhuri, N.P. Bhattacharyya, Identification of HYPK-interacting proteins reveals involvement of HYPK in regulating cell growth, cell cycle, unfolded protein response and cell death, PLoS ONE 7 (2012) e51415.
[14] S. Raychaudhuri, M. Sinha, D. Mukhopadhyay, N.P. Bhattacharyya, HYPK, a Huntingtin interacting protein, reduces aggregates and apoptosis induced by N-terminal Huntingtin with 40 glutamines in Neuro2a cells and exhibits chaperone-like activity, Hum. Mol. Genet. 17 (2008) 240–255.
[15] M. Sinha, J. Ghose, N.P. Bhattarcharyya, Micro RNA-214,-150,-146a and-125b target Huntingtin gene, RNA Biol. 8 (2011) 1005–1021.
[16] E. Rockabrand, N. Slepko, A. Pantalone, V.N. Nukala, A. Kazantsev, J.L. Marsh, P.G. Sullivan, J.S. Steffan, S.L. Sensi, L.M. Thompson, The first 17 amino acids of Huntingtin modulate its sub-cellular localization, aggregation and effects on calcium homeostasis, Hum. Mol. Genet. 16 (2007) 61–77.
[17] R.S. Atwal, J. Xia, D. Pinchev, J. Taylor, R.M. Epand, R. Truant, Huntingtin has a membrane association signal that can modulate Huntingtin aggregation, nuclear entry and toxicity, Hum. Mol. Genet. 16 (2007) 2600–2615.
[18] Z.H. Qin, Y. Wang, E. Sapp, B. Cuiffo, E. Wanker, M.R. Hayden, K.B. Kegel, N. Aronin, M. DiFiglia, Huntingtin bodies sequester vesicle-associated proteins by a polyproline-dependent interaction, J. Neurosci. 24 (2004) 269–281.
[19] S. Tam, C. Spiess, W. Auyeung, L. Joachimiak, B. Chen, M.A. Poirier, J. Frydman, The chaperonin TRiC blocks a Huntingtin sequence element that promotes the conformational switch to aggregation, Nat. Struct. Mol. Biol. 16 (2009) 1279–1285.
[20] E. Scherzinger, A. Sittler, K. Schweiger, V. Heiser, R. Lurz, R. Hasenbank, G.P. Bates, H. Lehrach, E.E. Wanker, Self-assembly of polyglutamine-containing Huntingtin fragments into amyloid-like fibrils: implications for Huntington's disease pathology, Proc. Natl. Acad. Sci. U.S.A. 96 (1999) 4604–4609.
[21] R. Kayed, E. Head, J.L. Thompson, T.M. McIntire, S.C. Milton, C.W. Cotman, C.G. Glabe, Common structure of soluble amyloid oligomers implies common mechanism of pathogenesis, Science 300 (2003) 486–489.
[22] M. Arrasate, S. Mitra, E.S. Schweitzer, M.R. Segal, S. Finkbeiner, Inclusion body formation reduces levels of mutant Huntingtin and the risk of neuronal death, Nature 431 (2004) 805–810.
[23] R. Kayed, Y. Sokolov, B. Edmonds, T.M. McIntire, S.C. Milton, J.E. Hall, C.G. Glabe, Permeabilization of lipid bilayers is a common conformation-dependent activity of soluble amyloid oligomers in protein misfolding diseases, J. Biol. Chem. 279 (2004) 46363–46366.
[24] S.W. Liebman, S.C. Meredith, Protein folding: sticky N17 speeds Huntingtin pile-up, Nat. Chem. Biol. 6 (2010) 7–8.